NASA Technical Paper 3291

CECOM Technical Report 92-E-5

December 1992

Scattering From Arbitrarily Shaped Microstrip Patch Antennas

David G. Shively,
Manohar D. Deshpande,
and Capers R. Cockrell

NASA Technical Paper 3291

CECOM Technical Report 92-E-5

1992

Scattering From Arbitrarily Shaped Microstrip Patch Antennas

David G. Shively
Joint Research Program Office
Electronics Integration Directorate
Communications Electronics Command
Langley Research Center
Hampton, Virginia

Manohar D. Deshpande
ViGYAN, Inc.
Hampton, Virginia

Capers R. Cockrell
Langley Research Center
Hampton, Virginia

REPORT DOCUMENTATION PAGE

Form Approved
OMB No. 0704-0188

1. AGENCY USE ONLY *(Leave blank)*	2. REPORT DATE	3. REPORT TYPE AND DATES COVERED
	December 1992	Technical Paper

4. TITLE AND SUBTITLE
Scattering From Arbitrarily Shaped Microstrip Patch Antennas

5. FUNDING NUMBERS
PR 1L161102AH45
WU 505-64-52-60

6. AUTHOR(S)
David G. Shively, Manohar D. Deshpande, and Capers R. Cockrell

7. PERFORMING ORGANIZATION NAME(S) AND ADDRESS(ES)
NASA Langley Research Center
Hampton, VA 23681-0001

Joint Research Program Office
Electronics Integration Directorate
Communications Electronics Command
Langley Research Center
Hampton, VA 23681-0001

8. PERFORMING ORGANIZATION REPORT NUMBER
L-17122

9. SPONSORING/MONITORING AGENCY NAME(S) AND ADDRESS(ES)
National Aeronautics and Space Administration
Washington, DC 20546-0001
and
U.S. Army Communications Electronics Command
Fort Monmouth, NJ 07703-5603

10. SPONSORING/MONITORING AGENCY REPORT NUMBER
NASA TP-3291
CECOM TR-92-E-5

11. SUPPLEMENTARY NOTES
Shively: EID-CECOM, Hampton, VA; Deshpande: ViGYAN, Inc., VA; Cockrell: Langley Research Center, Hampton, VA.

12a. DISTRIBUTION/AVAILABILITY STATEMENT
Unclassified–Unlimited

Subject Category 32

12b. DISTRIBUTION CODE

13. ABSTRACT *(Maximum 200 words)*

The scattering properties of arbitrarily shaped microstrip patch antennas are examined. The electric field integral equation for a current element on a grounded dielectric slab is developed for a rectangular geometry based on Galerkin's technique with subdomain rooftop basis functions. A shape function is introduced that allows a rectangular grid approximation to the arbitrarily shaped patch. The incident field on the patch is expressed as a function of incidence angle θ^i, ϕ^i. The resulting system of equations is then solved for the unknown current modes on the patch, and the electromagnetic scattering is calculated for a given angle. Comparisons are made with other calculated results as well as with measurements.

14. SUBJECT TERMS	15. NUMBER OF PAGES
Antennas; Scattering; Microstrip; Moment method	33
	16. PRICE CODE: A03

17. SECURITY CLASSIFICATION OF REPORT	18. SECURITY CLASSIFICATION OF THIS PAGE	19. SECURITY CLASSIFICATION OF ABSTRACT	20. LIMITATION OF ABSTRACT
Unclassified	Unclassified		

ACKNOWLEDGMENTS

The authors would like to thank Kenna K. Macauley, Mason & Hanger Services Inc., for preparing the figures for this manuscript, and Erik Vedeler, Guidance and Control Division, for assisting with the measurements. Our appreciation is also extended to Dr. James T. Aberle, Arizona State University, for supplying the data for figures 3 and 4.

Abstract

The scattering properties of arbitrarily shaped microstrip patch antennas are examined. The electric field integral equation for a current element on a grounded dielectric slab is developed for a rectangular geometry based on Galerkin's technique with subdomain rooftop basis functions. A shape function is introduced that allows a rectangular grid approximation to the arbitrarily shaped patch. The incident field on the patch is expressed as a function of incidence angle θ^{i}, ϕ^{i}. The resulting system of equations is then solved for the unknown current modes on the patch, and the electromagnetic scattering is calculated for a given angle. Comparisons are made with other calculated results as well as with measurements.

Introduction

In the early 1980's, the moment method technique was developed for analyzing microstrip patch antennas by using the spectral domain Green's function. This technique accurately accounts for dielectric thickness, dielectric losses, and surface wave losses and can be extended to include the effects of a cover layer with a different dielectric constant on top of the antenna. Because of its spectral nature, the technique can be easily extended to model an infinite array of patches by the examination of only a single unit cell.

Early papers on this subject include those by Bailey and Deshpande (refs. 1 to 3) and Pozar (ref. 4). In those papers the authors used both subdomain and entire-domain basis functions to model the current on the patch. Results such as bandwidth, input impedance, and resonant frequency were presented for rectangular patches. The use of subdomain basis functions yields more flexibility in the modeling of the patch current, whereas the use of entire-domain basis functions yields a smaller number of unknowns in the solution. For this reason, many subsequent analyses involve entire-domain basis functions that are limited to canonical shapes such as rectangles, circles, and ellipses. Using entire-domain basis functions, Pozar and Schaubert (ref. 5) extended the method from a single patch to an infinite array of patches. Aberle and Pozar (refs. 6 and 7) analyzed circular microstrip patch antennas, in both single and array geometries, using entire-domain basis functions. Bailey and Deshpande (ref. 8) also used entire-domain basis functions in their study of elliptical and circular patches. Aberle and Pozar (refs. 9 and 10) have improved on the original idealized probe feed model by including attachment modes of current that accurately model the current singularity at the probe feed point.

Recently, much work has been published regarding the scattering properties of microstrip antennas on various types of substrate geometries. Virtually all this work has been done with entire-domain basis functions for the current on the patch. Newman and Forrai (ref. 11) have analyzed the electromagnetic scattering from a rectangular patch. Jackson (ref. 12) extended this research to include a superstrate covering the antenna. Pozar (ref. 13) examined a patch on a uniaxial substrate. Aberle, Pozar, and Birtcher (ref. 14) included the improved probe feed model for analyzing the scattering from circular patches.

Some work has been published concerning the use of subdomain basis functions for modeling the current on the patch antenna. Most of this work was done in the spatial domain and cannot be extended to infinite arrays as in the spectral domain approach. Hall and Mosig (refs. 15 and 16) have analyzed rectangular microstrip antennas using a mixed-potential integral equation with subdomain rooftop basis functions. Mosig (ref. 17) has also used this approach

to analyze patch antennas of arbitrary shape. Michalski and Zheng (ref. 18) have used a similar formulation with triangular-surface patch basis functions, which are similar to finite element techniques, to model patches of arbitrary shape. Martinson and Kuester (ref. 19) have used a network approach along the edge of the patch to examine different shapes. As with the spatial domain method, this approach is not easily extended to array geometries. Hansen and Janhsen (ref. 20) have outlined a spectral domain approach that uses subdomain basis functions for modeling rectangular patches with a microstrip line-feed network.

This paper describes spectral domain analyses of arbitrarily shaped microstrip patch antennas in which subdomain basis functions are used to model the patch current. To simplify the analyses, the antenna feed will not be considered. The antenna is considered to be open circuited from the feed network (i.e., the feed impedance is infinite). Results are presented in the form of scattering as a function of frequency for a few representative shapes. Comparisons are made with measured data and with results from other analysis techniques.

Symbols

d	thickness of the dielectric slab
E_b	electric field radiated by a current element on the patch
E_θ	$\widehat{\boldsymbol{\theta}}$ component of the electric field
E_ϕ	$\widehat{\boldsymbol{\phi}}$ component of the electric field
$\mathbf{E}_{\tan}^{\text{inc}}$	tangential components of the incident electric field
$\mathbf{E}_{\tan}^{\text{scat}}$	tangential components of the scattered electric field
F^{mn}	Fourier transform of current mode mn
$\overleftrightarrow{\mathbf{G}}$	dyadic Green's function
$G_{ab}(x, y, z)$	component of the spatial domain Green's function
$G_{ab}(K_x, K_{y,z})$	component of the spectral domain Green's function
I^{mn}	amplitude of mode mn
$\mathbf{J}$	surface current on the microstrip patch antenna
j	$= \sqrt{-1}$
K, α	variables of integration in cylindrical coordinates
K_o	propagation constant for free space, $2\pi/\lambda_o$
K_x	spectral domain transformation variable for the x-direction
K_y	spectral domain transformation variable for the y-direction
K_1	propagation constant for the dielectric slab in the z-direction
K_2	propagation constant for free space in the z-direction
L_x	dimension of the patch in the x-direction
L_y	dimension of the patch in the y-direction
M	number of subdivisions in the x-direction
N	number of subdivisions in the y-direction

T_e	characteristic equation for transverse electric modes
T_m	characteristic equation for transverse magnetic modes
V^{pq}	component of excitation voltage vector
x, y, z	coordinates of the field point
x_m, y_n	coordinates of the current mode mn
x_o, y_o, z_o	coordinates of the source point
$\widehat{\mathbf{x}}$	unit vector in the x-direction
$\widehat{\mathbf{y}}$	unit vector in the y-direction
Z	impedance matrix to be solved
Z_o	impedance of free space, 377 ohms
$\widehat{\mathbf{z}}$	unit vector in the z-direction
β	$= \sqrt{K_x^2 + K_y^2}$
Δx	cell size in the x-direction
Δy	cell size in the y-direction
ε_r	relative permittivity of the dielectric slab
$\boldsymbol{\theta}^i$, $\boldsymbol{\phi}^i$	incident angle of electromagnetic wave
Λ	piecewise linear function for the current on the patch
μ_o	permeability of free space
Π	pulse function for the current on the patch
$\sigma_{\theta\theta}$	$\widehat{\boldsymbol{\theta}}$ polarized backscatter from $\widehat{\boldsymbol{\theta}}$ polarized incident field
ω	frequency of the electromagnetic field, rad

Abbreviation:

dBsm	a unit denoting decibels referenced to square meters

Theory

The geometry of a rectangular microstrip patch antenna is shown in figure 1. The patch is on a grounded dielectric slab of infinite extent. The dielectric slab has a relative permittivity ε_r and thickness d. Assuming that the patch is perfectly conducting, the boundary condition on the patch is given by

$$\mathbf{E}_{\tan}^{\text{inc}} = -\mathbf{E}_{\tan}^{\text{scat}} \tag{1}$$

The incident field is the field at the patch location attributable either to an incident plane wave or a probe or stripline feed. The scattered field is found from the currents excited on the patch as

$$\mathbf{E}^{\text{scat}}(x, y, z) = \iiint \overleftrightarrow{\mathbf{G}}(x, y, z|x_o, y_o, z_o) \cdot \mathbf{J}(x_o, y_o, z_o)\, dx_o dy_o dz_o \tag{2}$$

where $\overleftrightarrow{\mathbf{G}}$ is the dyadic Green's function for a current element on a grounded dielectric slab and $\mathbf{J}$ is the electric current density for the unknown vector on the patch. The dyadic Green's function can be written as

$$\overleftrightarrow{\mathbf{G}} = \widehat{\mathbf{x}}G_{xx}\widehat{\mathbf{x}} + \widehat{\mathbf{x}}G_{xy}\widehat{\mathbf{y}} + \widehat{\mathbf{x}}G_{xz}\widehat{\mathbf{z}} + \widehat{\mathbf{y}}G_{yx}\widehat{\mathbf{x}} + \widehat{\mathbf{y}}G_{yy}\widehat{\mathbf{y}} + \widehat{\mathbf{y}}G_{yz}\widehat{\mathbf{z}} + \widehat{\mathbf{z}}G_{zx}\widehat{\mathbf{x}} + \widehat{\mathbf{z}}G_{zy}\widehat{\mathbf{y}} + \widehat{\mathbf{z}}G_{zz}\widehat{\mathbf{z}} \tag{3}$$

where

$$G_{ab} = \frac{1}{4\pi^2} \int_{-\infty}^{\infty} \int_{-\infty}^{\infty} \widetilde{G}_{ab}\left(K_x, K_y, z|z_o\right) \exp\left[jK_x\left(x - x_o\right)\right] \exp\left[jK_y\left(y - y_o\right)\right] dK_x dK_y \qquad (4)$$

and a and b can be x, y, or z. Note that the components for the Green's function $\widetilde{G}_{ab}$ are known in the spectral domain and must be transformed back to the x, y domain; hence, the two infinite integrals in equation (4) are required.

The components of the Green's function are given by

$$\widetilde{G}_{xx}\left(K_x, K_y, d|d\right) = \frac{-jZ_o}{K_o} \frac{K_1 K_2 K_x^2 T_e + K_o^2 K_y^2 T_m}{\beta^2 T_m T_e} \sin\left(K_1 d\right) \qquad (5)$$

$$\widetilde{G}_{xy}\left(K_x, K_y, d|d\right) = \frac{-jZ_o}{K_o} \frac{K_x K_y \left(K_o^2 T_m - K_1 K_2 T_e\right)}{\beta^2 T_m T_e} \sin\left(K_1 d\right) \qquad (6)$$

$$\widetilde{G}_{yx}\left(K_x, K_y, d|d\right) = \widetilde{G}_{xy}\left(K_x, K_y, d|d\right) \qquad (7)$$

$$\widetilde{G}_{yy}\left(K_x, K_y, d|d\right) = \frac{-jZ_o}{K_o} \frac{K_1 K_2 K_y^2 T_e + K_o^2 K_x^2 T_m}{\beta^2 T_m T_e} \sin\left(K_1 d\right) \qquad (8)$$

$$\widetilde{G}_{zx} = \frac{-jZ_o}{K_o} \frac{K_x K_1}{T_m} \sin\left(K_1 d\right) \qquad (9)$$

$$\widetilde{G}_{zy} = \frac{-jZ_o}{K_o} \frac{K_y K_1}{T_m} \sin\left(K_1 d\right) \qquad (10)$$

where

$$T_m = \varepsilon_r K_2 \cos\left(K_1 d\right) + jK_1 \sin\left(K_1 d\right) \qquad (11)$$

$$T_e = K_1 \cos\left(K_1 d\right) + jK_2 \sin\left(K_1 d\right) \qquad (12)$$

$$K_1 = \sqrt{\varepsilon_r K_o^2 - \beta^2} \qquad Im\left(K_1\right) \leq 0 \qquad (13)$$

$$K_2 = \sqrt{K_o^2 - \beta^2} \qquad Im\left(K_2\right) \leq 0 \qquad (14)$$

$$\beta = \sqrt{K_x^2 + K_y^2} \qquad (15)$$

The remaining terms of the Green's function are not needed in this analysis. Details of the derivation of the Green's function can be found in reference 3. Additional forms of the Green's function that include the effects of a dielectric cover layer above the antenna are available in reference 10.

The current density **J** is modeled as a summation of piecewise linear subdomain basis functions known as rooftop basis functions. This approach contrasts with use of the entire-domain basis functions that span the entire patch. Entire-domain basis functions, such as sines and cosines, are useful for analyzing rectangular or circular patches, but become cumbersome for other shapes. Mathematically, the subdomain basis functions for the components of the current are described as

$$J_x(x,y) = \sum_{m=1}^{M} \sum_{n=1}^{N+1} I_x^{mn} \Lambda_m(x)\, \Pi_n(y) \tag{16}$$

$$J_y(x,y) = \sum_{m=1}^{M+1} \sum_{n=1}^{N} I_y^{mn} \Lambda_n(y)\, \Pi_m(x) \tag{17}$$

where the functions Λ and Π are "triangle" and "pulse" and are expressed as

$$\Lambda_m(x) = \begin{cases} 1 + (x - x_m)/\Delta x & (x_m - \Delta x) \le x \le x_m \\ 1 - (x - x_m)/\Delta x & x_m \le x \le (x_m + \Delta x) \\ 0 & \text{Otherwise} \end{cases} \tag{18}$$

$$\Pi_n(y) = \begin{cases} 1 & (y_n - \Delta y) \le y \le y_n \\ 0 & \text{Otherwise} \end{cases} \tag{19}$$

where $\Delta x = 2L_x/(M+1)$ and $\Delta y = 2L_y/(N+1)$.

When equations (2) and (4) are combined, the order of integration may be changed and the basis functions that represent the patch current density may be taken into the transform domain. These current density functions for the spectral domain are given by

$$\widetilde{\mathbf{J}}_x(K_x, K_y) = \sum_{m=1}^{M} \sum_{n=1}^{N+1} I_x^{mn} F_x^{mn}(K_x, K_y) \tag{20}$$

$$\widetilde{\mathbf{J}}_y(K_x, K_y) = \sum_{m=1}^{M+1} \sum_{n=1}^{N} I_y^{mn} F_y^{mn}(K_x, K_y) \tag{21}$$

where

$$F_x^{mn}(K_x, K_y) = \Delta x \Delta y \left[\frac{\sin(K_y \Delta y/2)}{K_y \Delta y/2}\right] \left[\frac{\sin(K_x \Delta x/2)}{K_x \Delta x/2}\right]^2 \exp[-jK_x x_m - jK_y y_n + jK_y(\Delta y/2)] \tag{22}$$

$$F_y^{mn}(K_x, K_y) = \Delta x \Delta y \left[\frac{\sin(K_y \Delta y/2)}{K_y \Delta y/2}\right]^2 \left[\frac{\sin(K_x \Delta x/2)}{K_x \Delta x/2}\right] \exp[-jK_x x_m - jK_y y_n + jK_x(\Delta x/2)] \tag{23}$$

Galerkin's method can be applied to the resulting equations to test them with the same set of basis functions. The solution yields a set of simultaneous equations that can be solved with standard techniques. Symbolically, this approach is represented as

$$\iint_S \mathbf{J}^{pq} \cdot \mathbf{E}_{\tan}^{\text{inc}}\, dxdy = -\iint_S \mathbf{J}^{pq} \cdot \mathbf{E}_{\tan}^{\text{scat}}\, dxdy \tag{24}$$

Note that the integration is over x and y instead of x_o and y_o. On the right side of equation (24) the x, y integration may be performed. The resulting Fourier transforms are similar to those described in equations (22) and (23). These equations can be shown in matrix notation as

$$\begin{bmatrix} V_x^{pq} \\ V_y^{pq} \end{bmatrix} = \begin{bmatrix} Z_{xx}^{pqmn} & Z_{xy}^{pqmn} \\ Z_{yx}^{pqmn} & Z_{yy}^{pqmn} \end{bmatrix} \begin{bmatrix} I_x^{mn} \\ I_y^{mn} \end{bmatrix} \tag{25}$$

where the impedance matrix terms are given by

$$Z_{xx}^{pqmn} = \frac{-1}{4\pi^2} \int_{-\infty}^{\infty} \int_{-\infty}^{\infty} \widetilde{G}_{xx}\left(K_x, K_y, d|d\right)\ F_x^{mn}\left(K_x, K_y\right)\ F_x^{pq}\left(-K_x, -K_y\right)\ dK_x dK_y \tag{26}$$

$$Z_{xy}^{pqmn} = \frac{-1}{4\pi^2} \int_{-\infty}^{\infty} \int_{-\infty}^{\infty} \widetilde{G}_{xy}\left(K_x, K_y, d|d\right)\ F_y^{mn}\left(K_x, K_y\right)\ F_x^{pq}\left(-K_x, -K_y\right)\ dK_x dK_y \tag{27}$$

$$Z_{yx}^{pqmn} = \frac{-1}{4\pi^2} \int_{-\infty}^{\infty} \int_{-\infty}^{\infty} \widetilde{G}_{yx}\left(K_x, K_y, d|d\right)\ F_x^{mn}\left(K_x, K_y\right)\ F_y^{pq}\left(-K_x, -K_y\right)\ dK_x dK_y \tag{28}$$

$$Z_{yy}^{pqmn} = \frac{-1}{4\pi^2} \int_{-\infty}^{\infty} \int_{-\infty}^{\infty} \widetilde{G}_{yy}\left(K_x, K_y, d|d\right)\ F_y^{mn}\left(K_x, K_y\right)\ F_y^{pq}\left(-K_x, -K_y\right)\ dK_x dK_y \tag{29}$$

The integrations in equations (26)–(29) must be done numerically but can be simplified with the following change of variables:

$$K_x = K\cos\alpha \qquad K_y = K\sin\alpha \tag{30}$$

With this change of variables, the integrals are changed to the form

$$\int_{-\infty}^{\infty} \int_{-\infty}^{\infty} [\qquad]\, dK_x dK_y = \int_0^{2\pi} \int_0^{\infty} [\qquad]\, K\, d\, K d\, \alpha \tag{31}$$

The integration from 0 to 2π may be further reduced to an integration from 0 to $\pi/2$ based on the even and odd properties of the integrand. Each of the four submatrices in the impedance matrix is of Toeplitz form, so only the first row of each submatrix needs to be calculated by numerical integration. The remaining terms can be filled in with these terms. Furthermore, because the impedance matrix terms $Z_{xy}^{pqmn} = Z_{yx}^{mnpq}$, even more computer time is saved.

To examine the scattering from a microstrip patch antenna, the left side of equation (25) must be evaluated. Each member of the excitation vector can be written as

$$V^{pq} = \iint_S \mathbf{J}^{pq} \cdot \mathbf{E}^{\text{inc}}\ dxdy \tag{32}$$

which is the incident field reacted with each pq current mode on the patch. After we use reciprocity, equation (32) can be rewritten as

$$V^{pq} = \frac{-4\pi \mathbf{E}^{pq} \cdot \mathbf{E}_o}{j\omega\mu_o} \tag{33}$$

In equation (33), $\mathbf{E}_o$ is the vector amplitude of the incident plane wave, $\mathbf{E}^{pq}$ is the far-field radiation from vector current mode pq on the patch, and $-4\pi/j\omega\mu_o$ is the required strength of an infinitesimal dipole source to produce a unit amplitude plane wave. The incident plane wave is from the direction $\boldsymbol{\theta}^i$, $\boldsymbol{\phi}^i$ in spherical coordinates with components E_θ and E_ϕ. Typical scattering results are of the form

$$\sigma_{\theta\theta} = 4\pi r^2 \ |E_\theta^{\text{scat}}|^2 \tag{34}$$

which is the $\widehat{\boldsymbol{\theta}}$ polarized backscatter from a unit amplitude $\widehat{\boldsymbol{\theta}}$ polarized incident field.

The fields radiated by a current mode on the patch can be found from the Green's function (see eq. (5)). The field at the point x, y, z from an $\widehat{\mathbf{x}}$ directed source located at the point x_o, y_o, d is given by

$$E_b(x,y,z) = \frac{1}{4\pi^2}\int_{-\infty}^{\infty}\int_{-\infty}^{\infty} \widetilde{G}_{bx} \ \exp\left[jK_x(x-x_o)\right] \ \exp\left[jK_y(y-y_o)\right] \ \exp\left[-jK_2(z-d)\right] dK_x dK_y \tag{35}$$

where b can be either x, y, or z. Likewise, the values x, y, z from a $\widehat{\mathbf{y}}$ directed source at point x_o, y_o, d are given by

$$E_b(x,y,z) = \frac{1}{4\pi^2}\int_{-\infty}^{\infty}\int_{-\infty}^{\infty} \widetilde{G}_{by} \ \exp\left[jK_x(x-x_o)\right] \ \exp\left[jK_y(y-y_o)\right] \ \exp\left[-jK_2(z-d)\right] dK_x dK_y \tag{36}$$

and again b can be either x, y, or z. These equations can be evaluated by the method of stationary phase and integrated over the extent of each basis function to give the fields radiated by that basis function in the presence of the grounded dielectric slab (ref. 13). After this evaluation has been done and the resulting equations are converted to spherical coordinates, the far-field components due to a single $\widehat{\mathbf{x}}$ directed current mode are

$$E_\theta^{mn}(r,\theta,\phi) = \frac{Z_o}{2\pi}\left[\frac{\exp(-jK_o r)}{r}\right] \ \exp(jK_2 d) \ \cos\ \theta \ \frac{K_1 K_o \ \cos\ \phi \ \sin(K_1 d)}{T_m} F_x^{mn}(K_x, K_y) \tag{37}$$

$$E_\phi^{mn}(r,\theta,\phi) = \frac{Z_o}{2\pi}\left[\frac{\exp(-jK_o r)}{r}\right] \ \exp(jK_2 d) \ \cos\ \theta \ \frac{-K_o^2 \ \sin\ \phi \ \sin(K_1 d)}{T_e} F_x^{mn}(K_x, K_y) \tag{38}$$

where K_x and K_y are evaluated at the stationary phase points

$$\left.\begin{aligned} K_x &= -K_o \ \sin\ \theta \ \cos\ \phi \\ K_y &= -K_o \ \sin\ \theta \ \sin\ \phi \end{aligned}\right\} \tag{39}$$

Similarly, the fields radiated by a single $\widehat{\mathbf{y}}$ directed current mode are given by

$$E_\theta^{mn}(r,\theta,\phi) = \frac{Z_o}{2\pi}\left[\frac{\exp(-jK_o r)}{r}\right] \ \exp(jK_2 d) \ \cos\ \theta \ \frac{K_1 K_o \ \sin\ \phi \ \sin(K_1 d)}{T_m} F_y^{mn}(K_x, K_y) \tag{40}$$

$$E_\phi^{mn}(r,\theta,\phi) = \frac{Z_o}{2\pi}\left[\frac{\exp(-jK_o r)}{r}\right] \ \exp(jK_2 d) \ \cos\ \theta \ \frac{K_o^2 \ \cos\ \phi \ \sin(K_1 d)}{T_e} F_y^{mn}(K_x, K_y) \tag{41}$$

where K_x and K_y are the same as in equation (39). By using equations (37) to (41) in equation (33), we can determine the left side of equation (25).

After the impedance matrix and the excitation vector have been calculated, the simultaneous equations can be solved for the unknown current coefficients. Then, the scattered fields can be

calculated by a summation of the radiated fields from each mode on the patch. If the patch is rectangular, this process is straightforward. However, if the patch is some other shape, additional steps are needed to model it properly.

Consider the irregular patch shown in figure 1. To predict the scattering from this patch, first enclose it within a rectangle. The impedance matrix and excitation vector can be calculated for this rectangular patch. A shape function is introduced that is equal to 1 for each mode that has its center point inside the irregularly shaped patch and equal to 0 if the center point of the mode is outside the irregularly shaped patch. The set of simultaneous equations can also be modified to consider only the modes for which the shape function is equal to 1. Thus, the boundary of the irregularly shaped patch is approximated by a rectangular grid or "stair step." As the number of subdivisions increases, the approximation to the true boundary of the patch improves. However, as the number of subdivisions increases, the time required to compute and solve the impedance matrix increases as well.

Results

Computer programs have been written to solve the matrix equation (25). These programs are listed in the appendix. The first program computes the elements of the impedance matrix by numerical integration. As mentioned previously, only the first row of each submatrix is calculated. The rest can be filled in by rearranging the first row. Also, because the Z_{xy} and Z_{yx} submatrices are related, only the Z_{xy} submatrix is calculated. The impedance matrix is then stored in a data file. The second program reads in the impedance matrix from the file and calculates the excitation vector for the given angle of incidence. The system of equations is solved and the electromagnetic scattering is calculated at the same angle. If scattering information is required over a band of frequencies, the third computer program reads in and arranges impedance matrices for several frequencies and computes the scattering at a given incidence angle as a function of frequency. It is necessary to compute only the impedance matrix at a few widely spaced frequencies because the impedance matrix terms are slow to change as a function of frequency. The impedance matrix for other frequencies can be found by an interpolation of each impedance matrix element. Newman and Forrai (ref. 11) have used this approach successfully with entire-domain basis functions.

To ensure that the computer programs are correct, comparisons are shown in figure 2 for the calculated and measured data presented by Newman and Forrai (ref. 11) and the calculated results from the subdomain technique. Because both the entire-domain basis functions used in reference 11 and the subdomain basis functions described here model the patch shape accurately, the calculated results from each technique should agree. The number of subdivisions here was chosen to be $M = N = 12$, which is adequate for modeling the patch across the frequency band. If frequency were further increased, more patch subdivisions would be necessary. Figure 2 shows the impedance matrix that was calculated through numerical integration at frequency steps of 400 MHz and that was interpolated at frequencies between these steps. A quadratic interpolation technique was used here as well as for the following results. Close agreement between the calculated results can be seen in figure 2; the only slight differences are at the peaks of the curves. Also, a slight offset in frequency is noted between the two calculations. However, this offset is not uncommon when two techniques are compared and is likely attributable to minor differences in the computer codes. The measured results shown in figure 2 agree well with the calculated results in some areas and disagree in others. Again, a slight frequency shift is noted when compared with the calculated results; this shift may indicate physical tolerances of the patch size, substrate thickness, or substrate dielectric parameters. At some points, the measured data agree better with the data from the subdomain technique; at other points, the measured data agree better with those from the entire-domain technique. In some areas, the

measured data do not agree with any calculated results; rapid fluctuations of the measured data in these instances suggest a problem with the measurement or calibration of the radar data.

Next, the shape function was included in the computer programs and two different circular microstrip patch antennas were modeled. In figure 3 calculated results for a circular patch modeled with subdomain basis functions are compared with results calculated by Aberle and Pozar (ref. 6) with entire-domain basis functions. The impedance matrix case for the subdomain basis function was calculated at 500-MHz steps and was interpolated elsewhere. For entire-domain basis functions, the patch boundary is a perfect circle; for the subdomain basis functions, the patch boundary only approximates a circle. As before, a slight frequency shift is noted between the two approaches. This shift can be attributed to slight differences between the two computer codes and the subdomain approximation of a circular boundary. The frequency shift increases as the frequency increases and is expected, as the difference between the true and approximated boundary is larger electrically as frequency increases. If the frequency shift is ignored, the two results are similar across the frequency band, especially from 2 to 4.5 GHz. Approximation of a circular boundary in the subdomain calculation may explain the slight differences in the relative power levels.

A second circular patch was modeled and compared with results from entire-domain calculations and with measured data. The entire-domain calculations and the measured data were supplied by Aberle, Pozar, and Birtcher (ref. 14) and are shown in figure 4. The agreement is fairly good between the subdomain, entire-domain, and measured data. Again, a slight frequency shift in the data is noted, as are slight differences in the values at the resonant peaks. For both patches, the number of subdivisions was chosen to be $M = N = 12$. More subdivisions were used for the latter patch to improve the agreement, but little improvement was noted.

Two other shapes, an equilateral triangle and a trapezoid, have been modeled with subdomain basis functions. As before, the impedance matrices were calculated at 500-MHz steps and were interpolated at other frequencies. For these two shapes no entire-domain basis function results have been reported. The measured data were collected in the Experimental Test Range at the Langley Research Center.

The calculated and measured results for the triangular microstrip patch antenna are shown in figure 5. As before, the number of subdivisions was chosen to be $M = N = 12$. As in all previous cases, a slight frequency shift is evident in the data and the peak values of the data are slightly different. The same rapid fluctuations in the measured data as in figure 2 are observed from 9 to 13 GHz; these fluctuations are caused by imperfections in the measurement and calibration process. The measured versus calculated results for the trapezoidal microstrip patch are shown in figure 6. Because the trapezoid is larger than the earlier examples, the number of subdivisions of the patch was changed to $M = 10$ and $N = 20$. Other combinations of M and N were tried with little change in the results.

The results in this case are not as good as in the previous cases. The shift in frequency between the calculated and measured data shown in figure 6 is larger than those in the previous cases. The relative power levels, however, are quite close for most peaks, although a large difference is evident at approximately 7.3 GHz. Rapid fluctuations in the measured data at that point suggest a measurement problem as the cause of the discrepancy.

Conclusions

A subdomain moment method technique has been developed to examine the scattering properties of microstrip patch antennas. Antennas of virtually any shape may now be analyzed with this technique merely by changing the shape function that defines the outer antenna boundary. Results were presented for rectangular, circular, triangular, and trapezoidal microstrip patch antennas. In all cases, slight shifts in frequency between subdomain, entire-domain, and measured

data were noted, as were slight differences in power level at the response peaks. The sub-domain calculations have, however, predicted the correct general scattering from all the patches examined.

NASA Langley Research Center
Hampton, VA 23681-0001
September 30, 1992

Appendix

Computer Programs That Solve Matrix Equation (25)

Evaluation of Z_{xx}, Z_{yy}, and Z_{xy} Submatrices

The following program computes the first row of the Z_{xx}, Z_{yy}, and Z_{xy} submatrices by numerical integration. The remaining terms of the impedance matrix are then filled and the matrix is stored in a data file.

```
ccccc Patch Impedance Matrix
ccccc Subdomain Basis Functions
ccccc
     program IMPEDANCE
     parameter(mm=12,nn=12,mmp1=(mm+1),nnp1=(nn+1))
     parameter(nmax1=(mm*nnp1),nmax2=(mmp1*nn),nmax=(nmax1+nmax2))
     real x(mmp1),y(nnp1),Lx,Ly,dx,dy,dx2,dy2,Dxy,d
     real Ko,fr,pi,pi2,s1,s2,epo,muo
     real B2,A2,DELTY2,FACTY2,FACTY1,FY2
     real alpha,ca,sa,deltyr,deltyi,YI1,YI2,ANG(60)
     integer NQ2,NUM,NS(60),Con(3)
     complex cj,er,Ke,tempx,tempy,P(60),FY1
     complex Gxx,Gxy,Gyy,sxx,sxy,syy,Txx,Tyy,Txy
     complex K,K1,K2,Tm,Te,N1,N2,D1,D2,C1,sd
     complex ZZ(nmax,nmax),DELTY1
     complex zxx(mmp1,nnp1,mmp1,nnp1),zxy(mmp1,nnp1,mmp1,nnp1)
     complex zyx(mmp1,nnp1,mmp1,nnp1),zyy(mmp1,nnp1,mmp1,nnp1)
     complex axx(mmp1,nnp1),axy(mmp1,nnp1),ayy(mmp1,nnp1)
     complex bxx(mmp1,nnp1),bxy(mmp1,nnp1),byy(mmp1,nnp1)
     DIMENSION U1(3),U2(10),R1(3),R2(10),U(13),R(13)
     EQUIVALENCE (U1(1),U(1)),(U2(1),U(4)),(R1(1),R(1)),(R2(1),R(4))
     DATA U1/.11270166537925,.5,.88729833462074/,U2/.01304673574141,.06
    1746831665550,.16029521585048,.28330230293537,.42556283050918,.5744
    23716949081,.71669769706462,.83970478414951,.93253168334449,.986953
    326425858/,R1/.27777777777777,.44444444444444,.27777777777777/,R2/.
    403333567215434,.07472567457529,.10954318125799,.13463335965499,.14
    5776211235737,.14776211235737,.13463335965499,.10954318125799,.0747
    62567457529,.03333567215434/
CCCCC
ccccc ALL DIMENSIONS IN METERS
ccccc
     cj=(0.0,1.0)
     pi=2.0*asin(1.0)
     pi2= pi/2.0
     epo= 8.854E-12
     muo= pi*(4.0E-07)
     er= cmplx(2.2,-0.0022)
     fr= 6.0E+09
     Ko= 2.0*pi*fr*sqrt(muo*epo)
     Ke= 2.0*pi*fr*csqrt(muo*epo*er)
     d= 0.00159
     Lx= 0.023
```

```
      Ly= 0.023
      dx=(2.0*Lx)/(float(mmp1))
      dy=(2.0*Ly)/(float(nnp1))
      dx2=dx/2.0
      dy2=dy/2.0
      Dxy= dx*dx*dy*dy
      do 3 i=1,mmp1
      x(i)= -Lx + (float(i)*dx)
     3 continue
      do 5 i=1,nnp1
      y(i)= -Ly + (float(i)*dy)
     5 continue
      write(6,10)Ko,Ke,Lx,Ly
    10 format('Ko=',f7.3,' Ke=',f7.3,f7.3,' Lx=',f9.6,' Ly=',f9.6)
      zxx=(0.0,0.0)
      zxy=(0.0,0.0)
      zyx=(0.0,0.0)
      zyy=(0.0,0.0)
      axx=(0.0,0.0)
      axy=(0.0,0.0)
      ayy=(0.0,0.0)
ccccc
ccccc Calculate Integrals for the Z matrix
ccccc
ccccc Define Limits for K integration
ccccc
      P(1)= (0.0,0.0)
      P(2)= cmplx((0.1*Ko),(0.1*Ko))
      P(3)= cmplx((1.0*Ko),(0.1*Ko))
      P(4)= cmplx((1.1*real(Ke)),(0.1*Ko))
      P(5)= cmplx((1.1*real(Ke)),(0.0))
      P(6)= cmplx((1.5*real(Ke)),0.0)
      P(7)= cmplx((4.0*real(Ke)),0.0)
      P(8)= cmplx((5.0*real(Ke)),0.0)
      do 11 n=9,60
      P(n)= float(n-8)*6000.0
    11 continue
      NS=50
      NS(1)=10
      NS(2)=20
      NS(3)=20
      NS(4)=10
      NS(5)=10
      NS(6)=40
      NS(7)=20
      NS(8)=100
ccccc
ccccc THETA Integration first
ccccc
      B2=pi2
      A2=0.0
```

```
      NQ2=6
      DELTY2= (B2-A2)/FLOAT(NQ2)
C*FIND INITIAL VALUE FOR THETA INTERVAL.
      DO 200 II=1,NQ2
      YI2 = float(II - 1)
      FY2 = A2 + (YI2*DELTY2)
CEVALUATE FUNCTIONS AT 10 POINTS PER THETA INTERVAL.
      DO 180 L2=1,10
      FACTY2=R(3+L2)
      alpha=FY2 + (U(3+L2)*DELTY2)
      ca=cos(alpha)
      sa=sin(alpha)
C
C NOW START K INTEGRATION
C
      Con=0
      Txx=(0.0,0.0)
      Txy=(0.0,0.0)
      Tyy=(0.0,0.0)
      DO 150 IS=1,59
      bxx=(0.0,0.0)
      bxy=(0.0,0.0)
      byy=(0.0,0.0)
      DELTY1= (P(IS+1)-P(IS))/FLOAT(NS(IS))
C*FIND INITIAL VALUE FOR K INTERVAL.
      DO 100 JJ=1,NS(IS)
      YI1 = float(JJ - 1)
      FY1 = P(IS) + (YI1*DELTY1)
CEVALUATE FUNCTIONS AT 10 POINTS PER K INTERVAL.
      DO 80 L1=1,10
      FACTY1=R(3+L1)
C
C Find K and evaluate Green's functions
C
      K=FY1 + (U(3+L1)*DELTY1)
      K1=csqrt((Ke**2)-(K**2))
      if (aimag(K1).gt.0.0) K1 = conjg(K1)
      K2=csqrt((Ko**2)-(K**2))
      if (aimag(K2).gt.0.0) K2 = conjg(K2)
      sd=csin(K1*d)
      Te= (K1*ccos(K1*d)) + (cj*K2*csin(K1*d))
      Tm= (er*K2*ccos(K1*d)) + (cj*K1*csin(K1*d))
      C1= ((cj*377.0*sd)/(Ko*Te*Tm))
      Gxx= (-C1) * ((K1*K2*ca*ca*Te) + (Ko*Ko*sa*sa*Tm))
      Gyy= (-C1) * ((K1*K2*sa*sa*Te) + (Ko*Ko*ca*ca*Tm))
      Gxy= C1 * ((Ko*Ko*ca*sa*Tm) - (K1*K2*ca*sa*Te))
C
C Evaluate Basis functions for each mode
C
      D1= dx2*K*ca
      N1= csin(D1)/D1
```

```
     D2= dy2*K*sa
     N2= csin(D2)/D2
C
C multiply by K for polar integration
C
     sxx= Gxx*K*FACTY1*Dxy*(N1**4)*(N2**2)
     sxy= Gxy*K*FACTY1*Dxy*(N1**3)*(N2**3)
     syy= Gyy*K*FACTY1*Dxy*(N1**2)*(N2**4)
C
C SET p and q = 1 and then vary m and n
C
     do 15 m=1,mmp1
     tempx= ccos(K*ca*(x(m)-x(1)))
     do 12 n=1,nnp1
     tempy= ccos(K*sa*(y(n)-y(1)))
     bxx(m,n)=(sxx*tempx*tempy) + bxx(m,n)
     byy(m,n)=(syy*tempx*tempy) + byy(m,n)
   12 continue
   15 continue
C
C Take abs() of dx and dy terms and do the sign later
C
     do 25 m=1,mmp1
     tempx= csin(K*ca*abs(x(1)-(x(m)-dx2)))
     do 20 n=1,nnp1
     tempy= csin(K*sa*abs(y(1)-dy2-y(n)))
     bxy(m,n)= (-1.0*sxy*tempx*tempy) + bxy(m,n)
   20 continue
   25 continue
ccccc write(6,75)K,(sxx/FACTY1)
   75 format(f12.5,f12.5,f15.12,f15.12)
   80 continue
  100 continue
     Txx=(bxx(1,1)*DELTY1) + Txx
     Txy=(bxy(1,1)*DELTY1) + Txy
     Tyy=(byy(1,1)*DELTY1) + Tyy
     axx= (bxx*DELTY1*FACTY2) + axx
     axy= (bxy*DELTY1*FACTY2) + axy
     ayy= (byy*DELTY1*FACTY2) + ayy
ccccc write(6,120)P(IS+1),(bxx(1,1)*DELTY1),Txx
  120 format(f10.2,f10.2,f13.10,f13.10,f13.10,f13.10)
     if (cabs(bxx(1,1)*DELTY1).lt.(0.02*cabs(Txx))) Con(1)=1
     if (cabs(bxy(1,1)*DELTY1).lt.(0.02*cabs(Txy))) Con(2)=1
     if (cabs(byy(1,1)*DELTY1).lt.(0.02*cabs(Tyy))) Con(3)=1
     if ((Con(1).eq.1).and.(Con(2).eq.1).and.(Con(3).eq.1)
     &.and.(IS.gt.16)) goto 170
  150 continue
  170 continue
ccccc write(6,175)(alpha*180.0/pi),P(IS+1)
  175 format(f12.2,f12.2,f12.2)
  180 continue
```

```
  200 continue
  202 format(f8.3,f8.3,f8.3,f8.3,f8.3,f8.3)
C
C Multiply by 4 for 1 quadrant integration
C Divide by 2pi*2pi for inverse Fourier transform
C Multiply by -1 for E in = - E scat
C
     axx= ((-1.0/(pi*pi))*axx*DELTY2)
     axy= ((-1.0/(pi*pi))*axy*DELTY2)
     ayy= ((-1.0/(pi*pi))*ayy*DELTY2)
C
C Now arrange the other matrices
C
     do 310 ip=1,mm
     do 310 iq=1,nnp1
     irow= ((ip-1)*nnp1) + iq
     do 300 m=1,mm
     do 300 n=1,nnp1
     icol= ((m-1)*nnp1) + n
     if ((ip.eq.1).and.(iq.eq.1)) then
       zxx(ip,iq,m,n)= axx(m,n)
      else
       mp=iabs(ip-m)+1
       nq=iabs(iq-n)+1
       zxx(ip,iq,m,n)= axx(mp,nq)
     endif
     ZZ(irow,icol)= zxx(ip,iq,m,n)
  300 continue
  310 continue
C
     do 360 ip=1,mm
     do 360 iq=1,nnp1
     irow= ((ip-1)*nnp1) + iq
     do 350 m=1,mmp1
     do 350 n=1,nn
     icol= ((m-1)*nn) + n + nmax1
     s1=sign(1.0,(x(ip)-(x(m)-dx2)))
     s2=sign(1.0,(y(iq)-dy2-y(n)))
     if ((ip.eq.1).and.(iq.eq.1)) then
       zxy(ip,iq,m,n)= axy(m,n)*s1*s2
      else
       mp=iabs(ip-m)+1
       if (m.lt.ip) mp=mp+1
       nq=iabs(iq-n)+1
       if (n.lt.iq) nq=nq-1
       zxy(ip,iq,m,n)= axy(mp,nq)*s1*s2
     endif
     ZZ(irow,icol)= zxy(ip,iq,m,n)
     zyx(m,n,ip,iq)=zxy(ip,iq,m,n)
  350 continue
  360 continue
```

```
C
     do 380 ip=1,mmp1
     do 380 iq=1,nn
     irow= ((ip-1)*nn) + iq + nmax1
     do 375 m=1,mm
     do 375 n=1,nnp1
     icol= ((m-1)*nnp1) + n
     ZZ(irow,icol)= zyx(ip,iq,m,n)
  375 continue
  380 continue
C
     do 400 ip=1,mmp1
     do 400 iq=1,nn
     irow= ((ip-1)*nn) + iq + nmax1
     do 400 m=1,mmp1
     do 400 n=1,nn
     icol= ((m-1)*nn) + n + nmax1
     if ((ip.eq.1).and.(iq.eq.1)) then
       zyy(ip,iq,m,n)= ayy(m,n)
      else
       mp=iabs(ip-m)+1
       nq=iabs(iq-n)+1
       zyy(ip,iq,m,n)= ayy(mp,nq)
     endif
     ZZ(irow,icol)= zyy(ip,iq,m,n)
  400 continue
C
ccccc     do 1200 m=1,nmax
ccccc     do 1200 n=1,nmax
ccccc     write(6,1100)m,n,ZZ(m,n)
ccccc 1100 format(i4,i4,f12.8,f12.8)
ccccc 1200 continue
     open(12,FILE='IMP',STATUS='NEW',FORM='UNFORMATTED')
     write(12)fr,Lx,dx,Ly,dy,d,Ko,Ke,er,x,y
     write(12)ZZ
     close(12)
 2000 stop
     end
ccccc
```

Solution for a Given Incidence Angle

The following program reads an impedance matrix data file, computes the excitation vector, and computes backscatter for a given incidence angle. The shape function is introduced and only those modes with a shape function equal to 1 are retained in the solution.

```
ccccc Microstrip Patch Matrix Inversion Code
     parameter (mm=12,nn=12,mmp1=(mm+1),nnp1=(nn+1))
     parameter (nmax1=(mm*nnp1),nmax2=(mmp1*nn),nmax=(nmax1+nmax2))
     real Lx,dx,Ly,dy,Ko,fr,x(mmp1),y(nnp1),px,py
     real pi,dx2,dy2,Theta,Phi,Kx,Ky,K2,F1,F2
     integer ipvt(nmax),Sx(mm,nnp1),Sy(mmp1,nn)
```

```
      complex er,Ke,axx,bxx,res,Rs,Di,Et,Ep,Ph
      complex cj,K1,Tm,Te,Ptx,Pty,Ppx,Ppy,Etx,Ety,Epx,Epy
      complex fac(nmax,nmax),wk(nmax)
      complex ZZ(nmax,nmax),V(nmax),Vx(nmax1),Vy(nmax2)
      complex ZZN(nmax,nmax),VN(nmax),Vmid,Jmid
      complex J(nmax)
      character*8 fn
      equivalence (Vx(1),V(1)),(Vy(1),V(nmax1+1))
      DIMENSION U1(3),U2(10),R1(3),R2(10),U(13),R(13)
      EQUIVALENCE (U1(1),U(1)),(U2(1),U(4)),(R1(1),R(1)),(R2(1),R(4))
      DATA U1/.11270166537925,.5,.88729833462074/,U2/.01304673574141,.06
     1746831665550,.16029521585048,.28330230293537,.42556283050918,.5744
     23716949081,.71669769706462,.83970478414951,.93253168334449,.986953
     326425858/,R1/.27777777777777,.44444444444444,.27777777777777/,R2/.
     403333567215434,.07472567457529,.10954318125799,.13463335965499,.14
     5776211235737,.14776211235737,.13463335965499,.10954318125799,.0747
     62567457529,.03333567215434/
C
      read(5,1)fn
     1format(A)
      open(12,file=fn,status='OLD',form='UNFORMATTED')
      read(12)fr,Lx,dx,Ly,dy,d,Ko,Ke,er,x,y
      read(12)ZZ
      close(12)
      write(6,2)fr,Lx,Ly,d,Ko,Ke,er
     2format(e10.3,f10.6,f10.6,f10.6,5f10.4)
      dx2=dx/2.0
      dy2=dy/2.0
      pi= 2.0*asin(1.0)
      cj= (0.0,1.0)
CCCCC
CCCCC Find Vx and Vy excitation for angle Theta and Phi
CCCCC
      Theta= 60.1*(pi/180.0)
      Phi= 0.1*(pi/180.0)
      Et= 1.0
      Ep= 0.0
      Kx= -Ko*sin(Theta)*cos(Phi)
      Ky= -Ko*sin(Theta)*sin(Phi)
      K1= csqrt((Ke**2)-(Kx**2)-(Ky**2))
      if (aimag(K1).gt.0.0) K1= conjg(K1)
      K2= Ko*cos(Theta)
      Tm= (er*K2*ccos(K1*d)) + (cj*K1*csin(K1*d))
      Te= (K1*ccos(K1*d)) + (cj*K2*csin(K1*d))
      Ptx= (K1*Ko*cos(Phi)*csin(K1*d))/Tm
      Pty= (K1*Ko*sin(Phi)*csin(K1*d))/Tm
      Ppx= -(Ko*Ko*sin(Phi)*csin(K1*d))/Te
      Ppy= (Ko*Ko*cos(Phi)*csin(K1*d))/Te
ccccc
      Di= -(4.0*pi)/(cj*2.0*pi*fr*pi*(4.0E-07))
      Etx= (377.0/(2.0*pi))*cexp(cj*K2*d)*cos(Theta)*Ptx
```

```
     Ety= (377.0/(2.0*pi))*cexp(cj*K2*d)*cos(Theta)*Pty
     Epx= (377.0/(2.0*pi))*cexp(cj*K2*d)*cos(Theta)*Ppx
     Epy= (377.0/(2.0*pi))*cexp(cj*K2*d)*cos(Theta)*Ppy
ccccc
     F1=dx*dy*(sin(Ky*dy2)/(Ky*dy2))*((sin(Kx*dx2)/(Kx*dx2))**2)
     F2=dx*dy*(sin(Kx*dx2)/(Kx*dx2))*((sin(Ky*dy2)/(Ky*dy2))**2)
     do 4 ip=1,mm
     do 3 iq=1,nnp1
     irow= ((ip-1)*nnp1) + iq
     Ph= cexp(cj*((-Kx*x(ip))+(-Ky*y(iq))+(Ky*dy2)))
     Vx(irow)= Di * ((Etx*Et)+(Epx*Ep)) *F1*Ph
     if ((ip.eq.6).and.(iq.eq.7)) Vmid=Vx(irow)
ccccc     write(6,10)ip,iq,Vx(irow)
    3 continue
    4 continue
     do 7 ip=1,mmp1
     do 6 iq=1,nn
     irow= ((ip-1)*nn) + iq
     Ph= cexp(cj*((-Kx*x(ip))+(-Ky*y(iq))+(Kx*dx2)))
     Vy(irow)= Di * ((Ety*Et)+(Epy*Ep)) *F2*Ph
ccccc     write(6,10)ip,iq,Vy(irow)
    6 continue
    7 continue
   10 format(i3,i3,f12.8,f12.8)
CCCCC
CCCCC Now define shape function
CCCCC
     Sx=1
     Sy=1
     do 550 m=1,mm
     do 540 n=1,nnp1
     dist=sqrt((x(m)**2)+((y(n)-dy2)**2))
     if (dist.gt.0.023) Sx(m,n)=0
  540 continue
  550 continue
     do 580 m=1,mmp1
     do 570 n=1,nn
     dist=sqrt(((x(m)-dx2)**2)+(y(n)**2))
     if (dist.gt.0.023) Sy(m,n)=0
  570 continue
  580 continue
     write(6,605)((Sx(m,n),m=1,mm),n=nnp1,1,-1)
  605 format(12I1)
     write(6,606)((Sy(m,n),m=1,mmp1),n=nn,1,-1)
  606 format(13I1)
     irownew=0
     do 650 ip=1,mm
     do 640 iq=1,nnp1
     icolnew=0
     if (Sx(ip,iq).eq.0) goto 640
     irow= ((ip-1)*nnp1) + iq
```

```
      irownew=irownew+1
      VN(irownew)=V(irow)
      do 620 m=1,mm
      do 610 n=1,nnp1
      if (Sx(m,n).eq.0) goto 610
      icol= ((m-1)*nnp1) + n
      icolnew=icolnew+1
      ZZN(irownew,icolnew)= ZZ(irow,icol)
  610 continue
  620 continue
      do 630 m=1,mmp1
      do 625 n=1,nn
      if (Sy(m,n).eq.0) goto 625
      icol= ((m-1)*nn) + n + nmax1
      icolnew=icolnew+1
      ZZN(irownew,icolnew)= ZZ(irow,icol)
  625 continue
  630 continue
  640 continue
  650 continue
      do 700 ip=1,mmp1
      do 690 iq=1,nn
      icolnew=0
      if (Sy(ip,iq).eq.0) goto 690
      irow= ((ip-1)*nn) + iq + nmax1
      irownew=irownew+1
      VN(irownew)= V(irow)
      do 660 m=1,mm
      do 655 n=1,nnp1
      if (Sx(m,n).eq.0) goto 655
      icol= ((m-1)*nnp1) + n
      icolnew=icolnew+1
      ZZN(irownew,icolnew)= ZZ(irow,icol)
  655 continue
  660 continue
      do 680 m=1,mmp1
      do 670 n=1,nn
      if (Sy(m,n).eq.0) goto 670
      icol= ((m-1)*nn) + n + nmax1
      icolnew= icolnew+1
      ZZN(irownew,icolnew)= ZZ(irow,icol)
  670 continue
  680 continue
  690 continue
  700 continue
      J=(0.0,0.0)
      write(6,720)irownew,icolnew
  720 format(i4,i4)
  750 call l2acg(irownew,ZZN,nmax,VN,1,J,fac,ipvt,wk)
ccccc     do 900 m=1,mm
ccccc     do 890 n=1,nnp1
```

```
ccccc     if (Sx(m,n).eq.0) goto 890
ccccc     mn=((m-1)*nnp1)+n
ccccc     write(6,800)m,n,Jx(mn),cabs(Jx(mn))
  800 format(i3,i3,f12.8,f12.8,f12.8)
  890 continue
  900 continue
ccccc     do 1000 m=1,mmp1
ccccc     do 990 n=1,nn
ccccc     if (Sy(m,n).eq.0) goto 990
ccccc     mn=((m-1)*nn)+n
ccccc     write(6,950)m,n,Jy(mn),cabs(Jy(mn))
  950 format(i3,i3,f12.8,f12.8,f12.8)
  990 continue
 1000 continue
CCCCC
CCCCC Now find RCS at angle (Theta,Phi)
CCCCC
     irow=0
     Et=(0.0,0.0)
     Ep=(0.0,0.0)
     do 1100 ip=1,mm
     do 1050 iq=1,nnp1
     if (Sx(ip,iq).eq.0) goto 1050
     irow= irow+1
     if ((ip.eq.6).and.(iq.eq.7)) Jmid=J(irow)
     Ph= cexp(cj*((-Kx*x(ip))+(-Ky*y(iq))+(Ky*dy2)))
     Et= Et+(J(irow)*Etx*F1*Ph)
     Ep= Ep+(J(irow)*Epx*F1*Ph)
 1050 continue
 1100 continue
     do 1200 ip=1,mmp1
     do 1150 iq=1,nn
     if (Sy(ip,iq).eq.0) goto 1150
     irow= irow+1
     Ph= cexp(cj*((-Kx*x(ip))+(-Ky*y(iq))+(Kx*dx2)))
     Et= Et+(J(irow)*Ety*F2*Ph)
     Ep= Ep+(J(irow)*Epy*F2*Ph)
 1150 continue
 1200 continue
 1300 format(i3,i3,f12.8,f12.8)
     RCS= 4.0*pi*cabs(Et)*cabs(Et)
     RCS= 10.0*alog10(RCS)
     write(6,1500)(fr/(1.0E+09)),RCS,(Jmid/Vmid)
 1400 format('Fr=',f6.2,' RCS = ',f12.6,' dBsm')
 1500 format(f8.4,f12.6,2x,e12.6,2x,e12.6)
 2000 continue
     stop
     end
ccccc
```

Solution for a Given Incidence Angle as a Function of Frequency

The following program reads impedance matrix data files and computes backscatter at a given incidence angle as a function of frequency. Quadratic interpolation is used to find the impedance matrix if the frequency of interest is between that of two data files. The shape function is included to ensure that only the appropriate modes are retained in the solution.

```
      program BANDWIDTH
      parameter (mm=12,nn=12,mmp1=(mm+1),nnp1=(nn+1))
      parameter (nmax1=(mm*nnp1),nmax2=(mmp1*nn),nmax=(nmax1+nmax2))
      parameter (NF=9)
      real Lx,dx,Ly,dy,Ko,fr,x(mmp1),y(nnp1)
      real pi,dx2,dy2,Theta,Phi,Kx,Ky,K2,F1,F2
      real f(NF),ZR(NF,nmax,nmax),ZI(NF,nmax,nmax),epo,muo
      real tempr(nmax,nmax),tempi(nmax,nmax),px1,px2,py1,py2
      real deltx,delty,ax,facty,factx,Tq,Tp,Tm1,Tn
      integer ipvt(nmax),Sx(mm,nnp1),Sy(mmp1,nn)
      complex er,Ke,Di,Et,Ep,Ph
      complex cj,K1,Tm,Te,Ptx,Pty,Ppx,Ppy,Etx,Ety,Epx,Epy
      complex fac(nmax,nmax),wk(nmax),ass,bxx,res
      complex ZZ(nmax,nmax),V(nmax),RR(nmax,nmax)
      complex J(nmax),JN
      complex ZZN(nmax,nmax),VN(nmax),Jmid,Vmid
      character*12 fn
      DIMENSION U1(3),U2(10),R1(3),R2(10),U(13),R(13)
      EQUIVALENCE (U1(1),U(1)),(U2(1),U(4)),(R1(1),R(1)),(R2(1),R(4))
      DATA U1/.11270166537925,.5,.88729833462074/,U2/.01304673574141,.06
     1746831665550,.16029521585048,.28330230293537,.42556283050918,.5744
     23716949081,.71669769706462,.83970478414951,.93253168334449,.986953
     326425858/,R1/.27777777777777,.44444444444444,.27777777777777/,R2/.
     403333567215434,.07472567457529,.10954318125799,.13463335965499,.14
     5776211235737,.14776211235737,.13463335965499,.10954318125799,.0747
     62567457529,.03333567215434/
C
      do 20 IF=1,NF
      if (IF.eq.1) fn='IMP6.0'
      if (IF.eq.2) fn='IMP6.5'
      if (IF.eq.3) fn='IMP7.0'
      if (IF.eq.4) fn='IMP7.5'
      if (IF.eq.5) fn='IMP8.0'
      if (IF.eq.6) fn='IMP8.5'
      if (IF.eq.7) fn='IMP9.0'
      if (IF.eq.8) fn='IMP9.5'
      if (IF.eq.9) fn='IMP10.0'
      if (IF.eq.10) fn='IMP10.5'
      if (IF.eq.11) fn='IMP11.0'
      if (IF.eq.12) fn='IMP11.5'
      if (IF.eq.13) fn='IMP12.0'
      if (IF.eq.14) fn='IMP12.5'
      if (IF.eq.15) fn='IMP13.0'
      if (IF.eq.16) fn='IMP13.5'
```

```
      if (IF.eq.17) fn='IMP14.0'
      open(12,file=fn,status='OLD',form='UNFORMATTED')
      read(12)fr,Lx,dx,Ly,dy,d,Ko,Ke,er,x,y
      read(12)ZZ
      close(12)
      f(IF)= fr
      do 10 m=1,nmax
      do 10 n=1,nmax
      ZR(IF,m,n)= real(ZZ(m,n))
      ZI(IF,m,n)= aimag(ZZ(m,n))
   10 continue
   20 continue
      dx2=dx/2.0
      dy2=dy/2.0
      pi= 2.0*asin(1.0)
      cj= (0.0,1.0)
      epo= 8.854E-12
      muo= pi*(4.0E-07)
CCCCC
CCCCC Start Freq. Loop
CCCCC
      do 2000 IF=2000,6000,25
      fr= (float(IF)/1000.0)*(1.0E+09)
      Ko= 2.0*pi*fr*sqrt(epo*muo)
      Ke= 2.0*pi*fr*csqrt(er*epo*muo)
      ipt= -1
      call inter(NF,NF,f,nmax,ZR,2,fr,tempr,ipt,ierr)
      ipt= -1
      call inter(NF,NF,f,nmax,ZI,2,fr,tempi,ipt,ierr)
      ZZ= cmplx(tempr,tempi)
CCCCC
CCCCC Find Vx and Vy excitation for angle Theta and Phi
CCCCC
      Theta= 60.0*(pi/180.0)
      Phi= 0.01*(pi/180.0)
      Et= 1.0
      Ep= 0.0
      Kx= -Ko*sin(Theta)*cos(Phi)
      Ky= -Ko*sin(Theta)*sin(Phi)
      K1= csqrt(cmplx(Ke**2)-(Kx**2)-(Ky**2))
      if (aimag(K1).gt.0.0) K1= conjg(K1)
      K2= Ko*cos(Theta)
      Tm= (er*K2*ccos(K1*d)) + (cj*K1*csin(K1*d))
      Te= (K1*ccos(K1*d)) + (cj*K2*csin(K1*d))
      Ptx= (K1*Ko*cos(Phi)*csin(K1*d))/Tm
      Pty= (K1*Ko*sin(Phi)*csin(K1*d))/Tm
      Ppx= -(Ko*Ko*sin(Phi)*csin(K1*d))/Te
      Ppy= (Ko*Ko*cos(Phi)*csin(K1*d))/Te
ccccc
      Di = -(4.0*pi)/(cj*2.0*pi*fr*muo)
      Etx= (377.0/(2.0*pi))*cexp(cj*K2*d)*cos(Theta)*Ptx
```

```
     Ety= (377.0/(2.0*pi))*cexp(cj*K2*d)*cos(Theta)*Pty
     Epx= (377.0/(2.0*pi))*cexp(cj*K2*d)*cos(Theta)*Ppx
     Epy= (377.0/(2.0*pi))*cexp(cj*K2*d)*cos(Theta)*Ppy
ccccc
     F1=dx*dy*(sin(Ky*dy2)/(Ky*dy2))*((sin(Kx*dx2)/(Kx*dx2))**2)
     F2=dx*dy*(sin(Kx*dx2)/(Kx*dx2))*((sin(Ky*dy2)/(Ky*dy2))**2)
     do 455 ip=1,mm
     do 454 iq=1,nnp1
     irow= ((ip-1)*nnp1) + iq
     Ph= cexp(cj*((-Kx*x(ip))+(-Ky*y(iq))+(Ky*dy2)))
     V(irow)= Di * ((Etx*Et)+(Epx*Ep)) *F1*Ph
     if ((ip.eq.6).and.(iq.eq.7)) Vmid=V(irow)
ccccc     write(6,470)ip,iq,V(irow)
  454 continue
  455 continue
     do 465 ip=1,mmp1
     do 460 iq=1,nn
     irow= ((ip-1)*nn) + iq + nmax1
     Ph= cexp(cj*((-Kx*x(ip))+(-Ky*y(iq))+(Kx*dx2)))
     V(irow)= Di * ((Ety*Et)+(Epy*Ep)) *F2*Ph
ccccc     if ((ip.eq.6).and.(iq.eq.6)) Vmid=V(irow)
ccccc     write(6,470)ip,iq,V(irow)
  460 continue
  465 continue
  470 format(i3,i3,f12.8,f12.8)
CCCCC
CCCCC Now define shape function
CCCCC
  500 Sx=1
     Sy=1
     do 550 m=1,mm
     do 540 n=1,nnp1
     dist=sqrt((x(m)**2)+((y(n)-dy2)**2))
     if (dist.gt.0.023) Sx(m,n)=0
  540 continue
  550 continue
     do 580 m=1,mmp1
     do 570 n=1,nn
     dist=sqrt(((x(m)-dx2)**2)+(y(n)**2))
     if (dist.gt.0.023) Sy(m,n)=0
  570 continue
  580 continue
     if (IF.eq.2000) write(6,605)((Sx(m,n),m=1,mm),n=nnp1,1,-1)
  605 format(12I1)
     if (IF.eq.2000) write(6,606)((Sy(m,n),m=1,mmp1),n=nn,1,-1)
  606 format(13I1)
     irownew=0
     do 650 ip=1,mm
     do 640 iq=1,nnp1
     icolnew=0
     if (Sx(ip,iq).eq.0) goto 640
```

```
      irow= ((ip-1)*nnp1) + iq
      irownew=irownew+1
      VN(irownew)=V(irow)
      do 620 m=1,mm
      do 610 n=1,nnp1
      if (Sx(m,n).eq.0) goto 610
      icol= ((m-1)*nnp1) + n
      icolnew=icolnew+1
      ZZN(irownew,icolnew)= ZZ(irow,icol)
  610 continue
  620 continue
      do 630 m=1,mmp1
      do 625 n=1,nn
      if (Sy(m,n).eq.0) goto 625
      icol= ((m-1)*nn) + n + nmax1
      icolnew=icolnew+1
      ZZN(irownew,icolnew)= ZZ(irow,icol)
  625 continue
  630 continue
  640 continue
  650 continue
      do 700 ip=1,mmp1
      do 690 iq=1,nn
      icolnew=0
      if (Sy(ip,iq).eq.0) goto 690
      irow= ((ip-1)*nn) + iq + nmax1
      irownew=irownew+1
      VN(irownew)= V(irow)
      do 660 m=1,mm
      do 655 n=1,nnp1
      if (Sx(m,n).eq.0) goto 655
      icol= ((m-1)*nnp1) + n
      icolnew=icolnew+1
      ZZN(irownew,icolnew)= ZZ(irow,icol)
  655 continue
  660 continue
      do 680 m=1,mmp1
      do 670 n=1,nn
      if (Sy(m,n).eq.0) goto 670
      icol= ((m-1)*nn) + n + nmax1
      icolnew= icolnew+1
      ZZN(irownew,icolnew)= ZZ(irow,icol)
  670 continue
  680 continue
  690 continue
  700 continue
      J=(0.0,0.0)
  750 call l2acg(irownew,ZZN,nmax,VN,1,J,fac,ipvt,wk)
CCCCC
CCCCC Now find RCS at angle (Theta,Phi)
CCCCC
```

```
      irow=0
      Et=(0.0,0.0)
      Ep=(0.0,0.0)
      do 1100 ip=1,mm
      do 1050 iq=1,nnp1
      if (Sx(ip,iq).eq.0) goto 1050
      irow= irow+1
ccccc     write(6,1040)float(ip),float(iq),cabs(J(irow))
 1040 format(f8.2,f8.2,f14.5)
      if ((ip.eq.6).and.(iq.eq.7)) Jmid=J(irow)
      Ph= cexp(cj*((-Kx*x(ip))+(-Ky*y(iq))+(Ky*dy2)))
      Et= Et+(J(irow)*Etx*F1*Ph)
      Ep= Ep+(J(irow)*Epx*F1*Ph)
 1050 continue
 1100 continue
      do 1200 ip=1,mmp1
      do 1150 iq=1,nn
      if (Sy(ip,iq).eq.0) goto 1150
      irow= irow+1
ccccc     write(6,1040)float(ip),float(iq),cabs(J(irow))
ccccc     if ((ip.eq.6).and.(iq.eq.6)) Jmid=J(irow)
      Ph= cexp(cj*((-Kx*x(ip))+(-Ky*y(iq))+(Kx*dx2)))
      Et= Et+(J(irow)*Ety*F2*Ph)
      Ep= Ep+(J(irow)*Epy*F2*Ph)
 1150 continue
 1200 continue
 1300 format(i3,i3,f12.8,f12.8)
      RCS= 4.0*pi*cabs(Et)*cabs(Et)
ccccc     RCS= 4.0*pi*cabs(Ep)*cabs(Ep)
      RCS= 10.0*alog10(RCS)
      JN=Jmid/Vmid
      write(6,1500)(fr/(1.0E+09)),RCS,JN
 1400 format('Fr=',f6.2,' RCS = ',f12.6,' dBsm')
 1500 format(f8.4,f12.6,2x,e12.6,2x,e12.6)
ccccc     write(6,1600)Vmid,Jmid
 1600 format(4e14.6)
 2000 continue
      stop
      end
ccccc
```

References

1. Bailey, M. C.; and Deshpande, M. D.: Integral Equation Formulation of Microstrip Antennas. *IEEE Trans. Antennas & Propag.,* vol. AP-30, no. 4, July 1982, pp. 651–656.

2. Deshpande, M. D.; and Bailey, M. C.: Input Impedance of Microstrip Antennas. *IEEE Trans. Antennas & Propag.,* vol. AP-30, no. 4, July 1982, pp. 645–650.

3. Bailey, M. C.; and Deshpande, M. D.: *Analysis of Rectangular Microstrip Antennas.* NASA TP-2276, 1984.

4. Pozar, David M.: Input Impedance and Mutual Coupling of Rectangular Microstrip Antennas. *IEEE Trans. Antennas & Propag.,* vol. AP-30, no. 6, Nov. 1982, pp. 1191–1196.

5. Pozar, David M.; and Schaubert, Daniel H.: Analysis of an Infinite Array of Rectangular Microstrip Patches With Idealized Probe Feeds. *IEEE Trans. Antennas & Propag.,* vol. AP-32, no. 10, Oct. 1984, pp. 1101–1107.

6. Aberle, J. T.; and Pozar, D. M.: Radiation and Scattering From Circular Microstrip Patches. *Antennas and Propagation*—1989 *IEEE APS International Symposium,* Volume I, IEEE Catalog No. CH-2654-2/89, IEEE Antennas and Propagation Soc., 1989, pp. 438–441.

7. Aberle, James T.; and Pozar, David M.: Analysis of Infinite Arrays of One- and Two-Probe-Fed Circular Patches. *IEEE Trans. Antennas & Propag.,* vol. 38, no. 4, Apr. 1990, pp. 421–432.

8. Bailey, M. C.; and Deshpande, M. D.: Analysis of Elliptical and Circular Microstrip Antennas Using Moment Method. *IEEE Trans. Antennas & Propag.,* vol. AP-33, no. 9, Sept. 1985, pp. 954–959.

9. Aberle, J. T.; and Pozar, D. M.: Analysis of Infinite Arrays of Probe-Fed Rectangular Microstrip Patches Using a Rigorous Feed Model. *IEE Proc., Part H: Microw., Antennas, & Propag.,* vol. 136, no. 2, Apr. 1989, pp. 110–119.

10. Aberle, James T.; and Pozar, David M.: Accurate and Versatile Solutions for Probe-Fed Microstrip Patch Antennas and Arrays. *Electromagnetics,*vol. 11, no. 1, Jan.–Mar. 1991, pp. 1–19.

11. Newman, Edward H.; and Forrai, David: Scattering From a Microstrip Patch. *IEEE Trans. Antennas & Propag.,* vol. AP-35, no. 3, Mar. 1987, pp. 245–251.

12. Jackson, David R.: The RCS of a Rectangular Microstrip Patch in a Substrate-Superstrate Geometry. *IEEE Trans. Antennas & Propag.,* vol. 38, no. 1, Jan. 1990, pp. 2–8.

13. Pozar, David M.: Radiation and Scattering From a Microstrip Patch on a Uniaxial Substrate. *IEEE Trans. Antennas & Propag.,* vol. AP-35, no. 6, June 1987, pp. 613–621.

14. Aberle, James T.; Pozar, David M.; and Birtcher, Craig R.: Evaluation of Input Impedance and Radar Cross Section of Probe-Fed Microstrip Patch Elements Using an Accurate Feed Model. *IEEE Trans. Antennas & Propag.,* vol. 39, no. 12, Dec. 1991, pp. 1691–1696.

15. Hall, Richard C.; and Mosig, Juan R.: The Analysis of Coaxially Fed Microstrip Antennas With Electrically Thick Substrates. *Electromagnetics,*vol. 9, 1989, pp. 367–384.

16. Hall, R. C.; and Mosig, J. R.: The Calculation of Mutual Coupling Between Microstrip Antennas With Thick Substrates. 1989 *International Symposium Digest—Antennas and Propagation,* Volume I, IEEE Catalog No. CH2654–2/89, IEEE Antennas and Propagation Soc., 1989, pp. 442–445.

17. Mosig, Juan R.: Arbitrarily Shaped Microstrip Structures and Their Analysis With a Mixed Potential Integral Equation. *IEEE Trans. Microw. Theory & Tech.,* vol. 36, no. 2, Feb. 1988, pp. 314–323.

18. Michalski, Krzysztof A.; and Zheng, Dalian: Analysis of Microstrip Resonators of Arbitrary Shape. *IEEE Trans. Microw. Theory & Tech.,* vol. 40, no. 1, Jan. 1992, pp. 112–119.

19. Martinson, Thomas M.; and Kuester, Edward F.: Accurate Analysis of Arbitrarily Shaped Patch Resonators on Thin Substrates. *IEEE Trans. Microw. Theory & Tech.,* vol. 36, no. 2, Feb. 1988, pp. 324–331.

20. Hansen, V.; and Janhsen, A.: Spectral Domain Analysis of Microstrip Arrays Including the Feed Network With Space-Varying Surface Impedances and Lumped Elements. *Electromagnetics,* vol. 11, no. 1, Jan.–Mar. 1991, pp. 69–88.

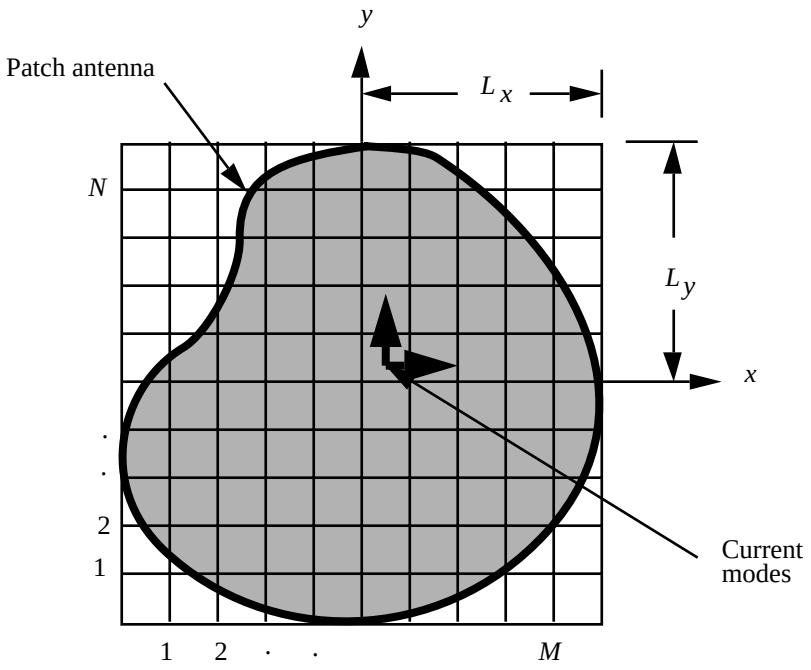

(a) Patch on a grounded slab of infinite extent.

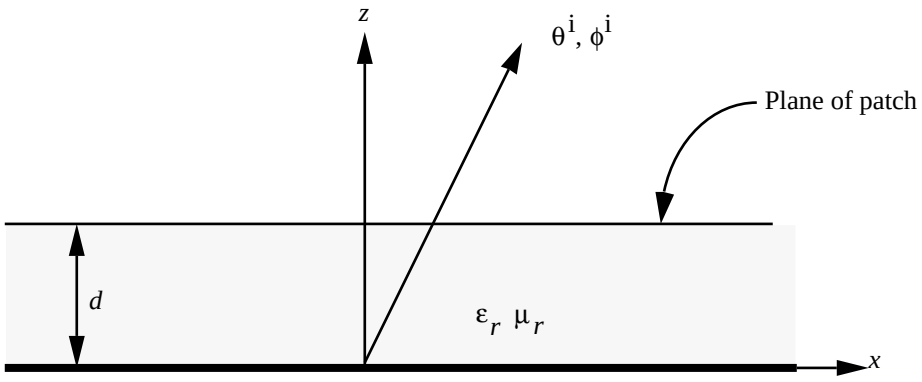

(b) Cross section of patch.

Figure 1. Geometry of an arbitrarily shaped microstrip patch antenna.

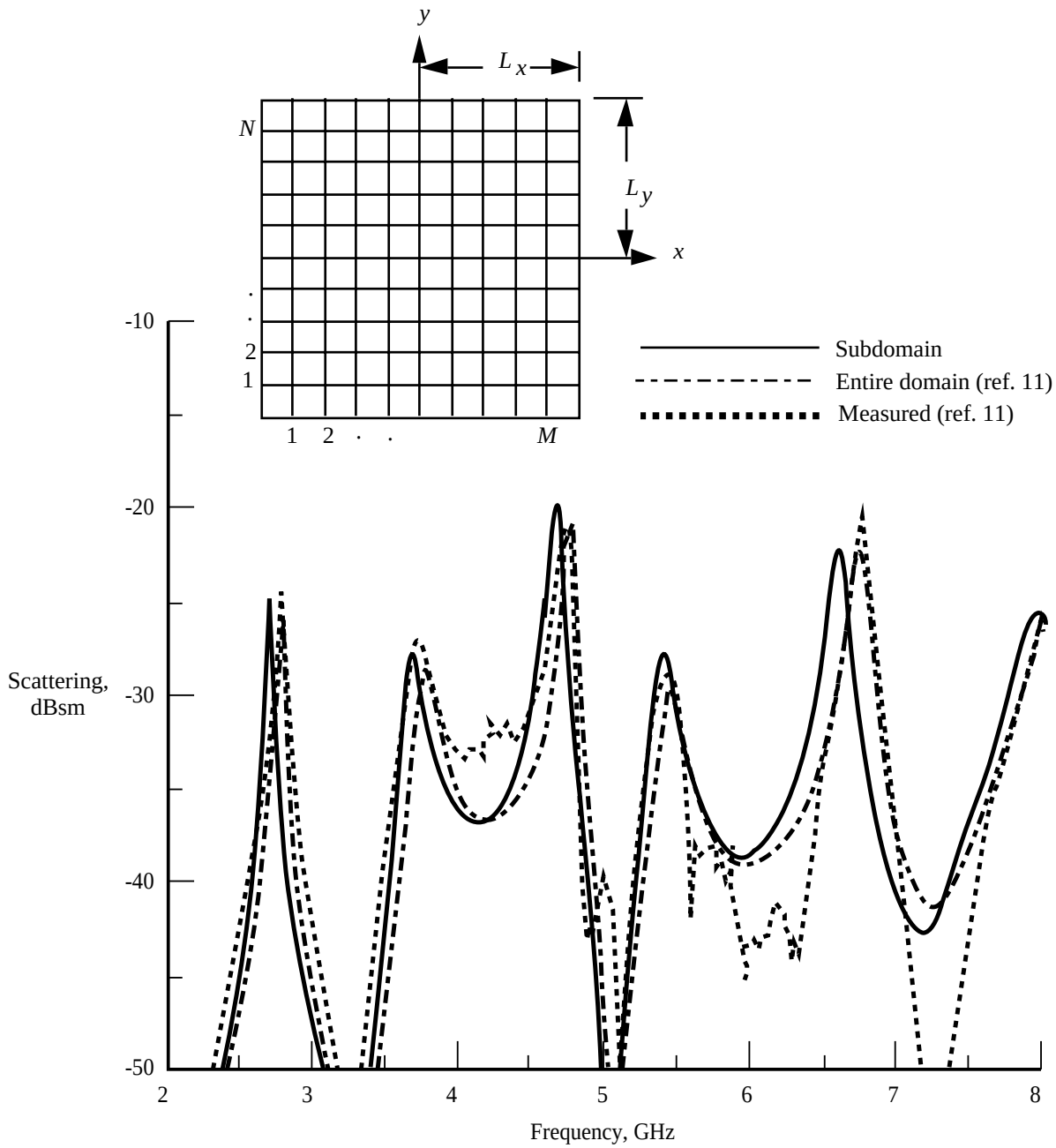

Figure 2. Comparison between subdomain, entire-domain, and measured scattering from a rectangular microstrip patch antenna. $L_x = 1.88$ cm; $L_y = 1.30$ cm; $d = 0.158$ cm; $\varepsilon_r = 2.17$; Loss tangent $= 0.001$; $\theta^i,\ \phi^i = 60°,\ 45°$.

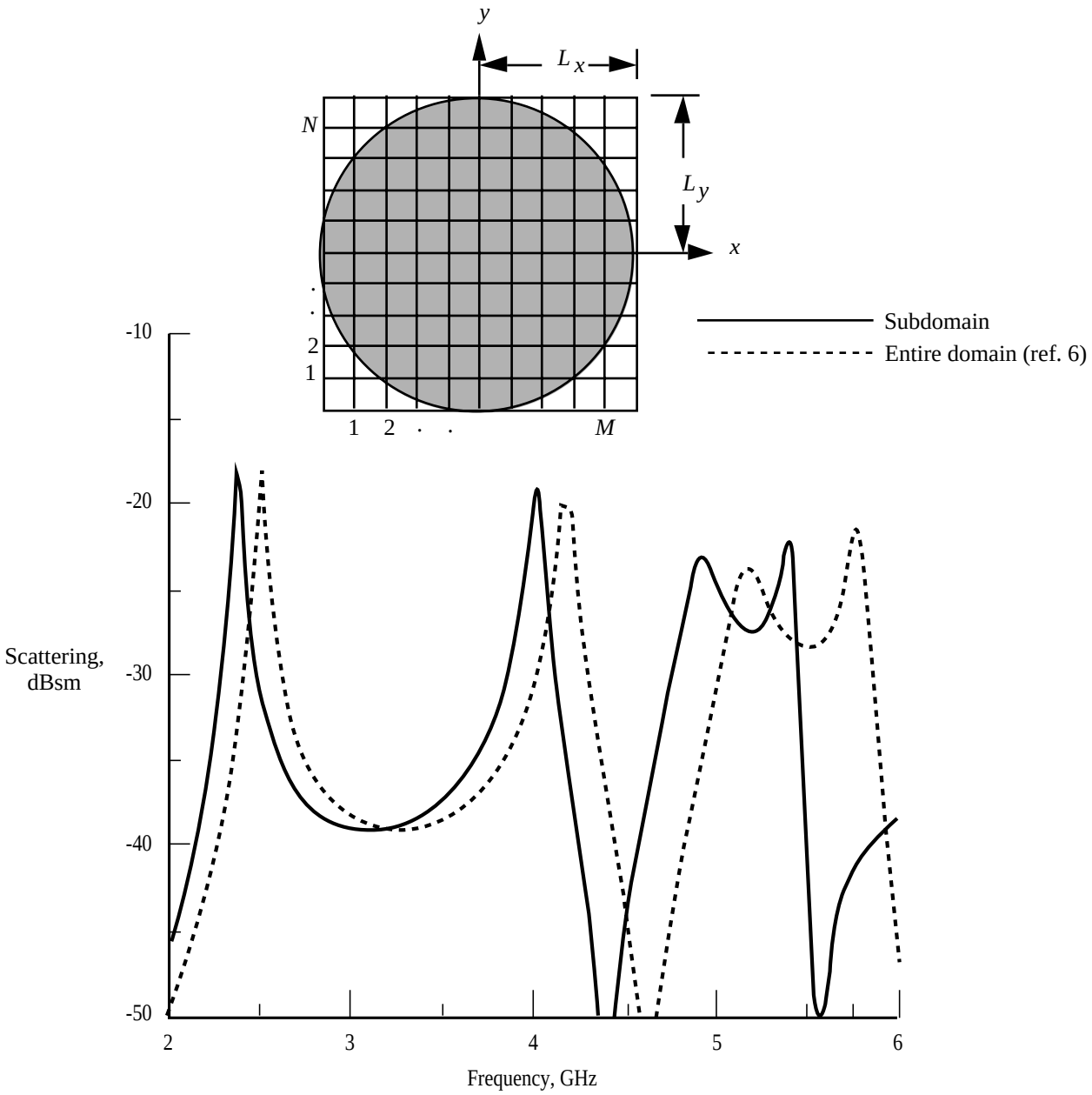

Figure 3. Comparison between subdomain and entire-domain calculated scattering from a circular microstrip patch antenna. Patch radius = 2.30 cm; d = 0.159 cm; ε_r = 2.20; Loss tangent = 0.0009; $\theta^i,\ \phi^i = 60°, 0°$.

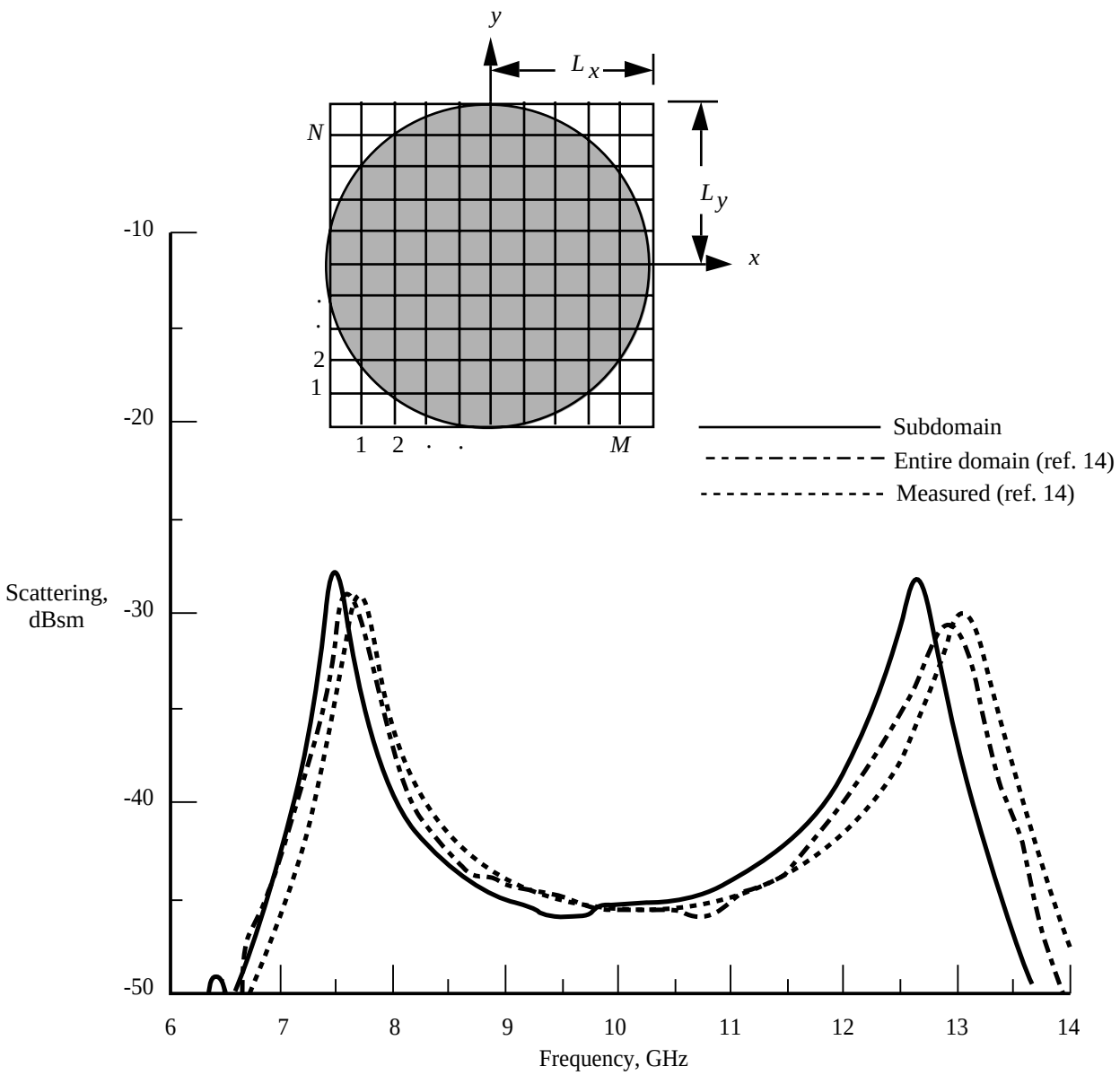

Figure 4. Comparison between subdomain; entire-domain, and measured scattering from a circular microstrip patch antenna. Patch radius = 0.71 cm; d = 0.07874 cm; ε_r = 2.20; Loss tangent = 0.0009; $\theta^i,\ \phi^i = 63°, 0°$.

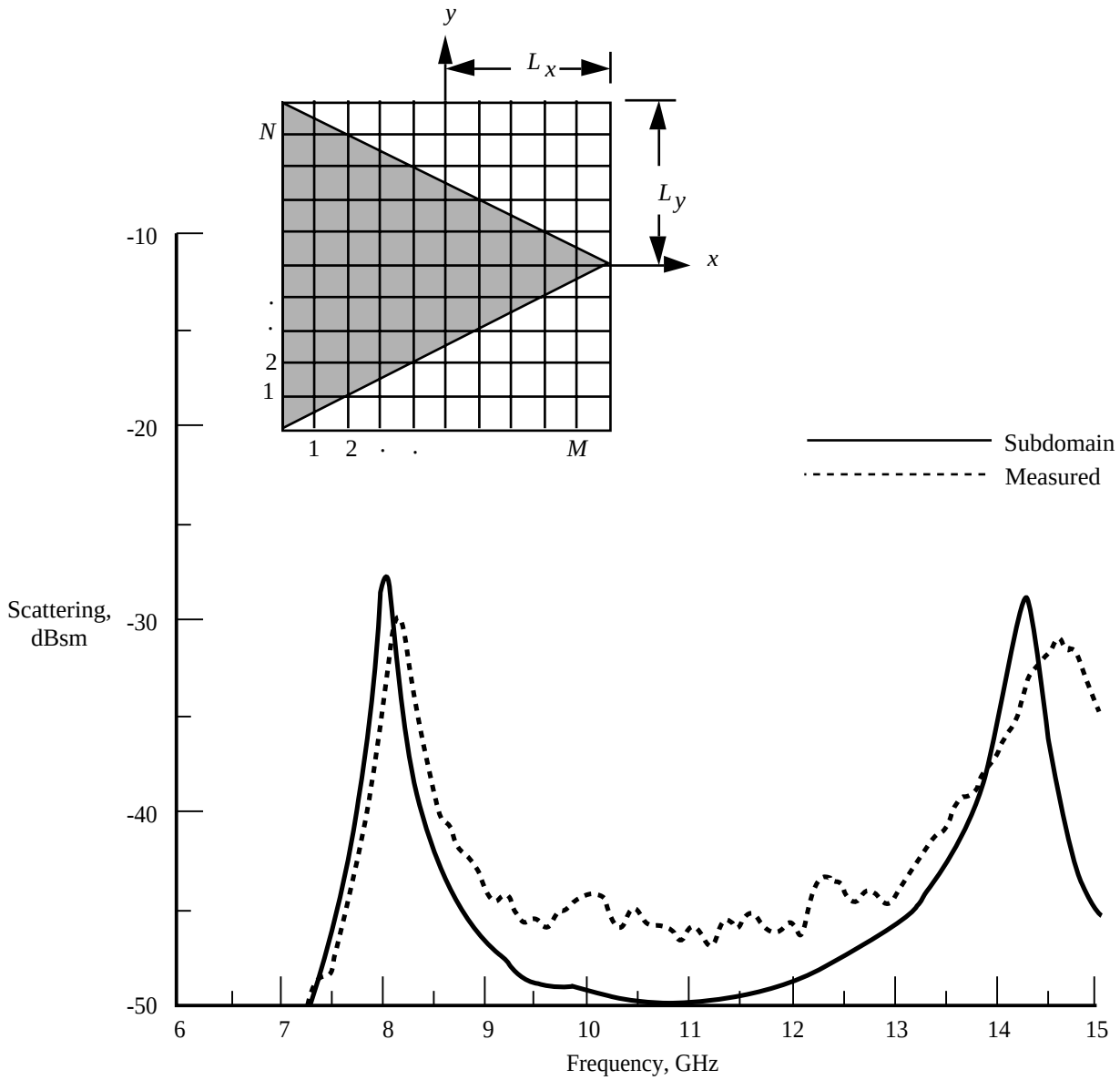

Figure 5. Comparison between subdomain and measured scattering from an equilateral triangle microstrip patch antenna. Triangle side = 1.4 cm; $d = 0.07874$ cm; $\varepsilon_r = 2.33$; Loss tangent $= 0.001$; $\theta^i,\ \phi^i = 60°, 180°$.

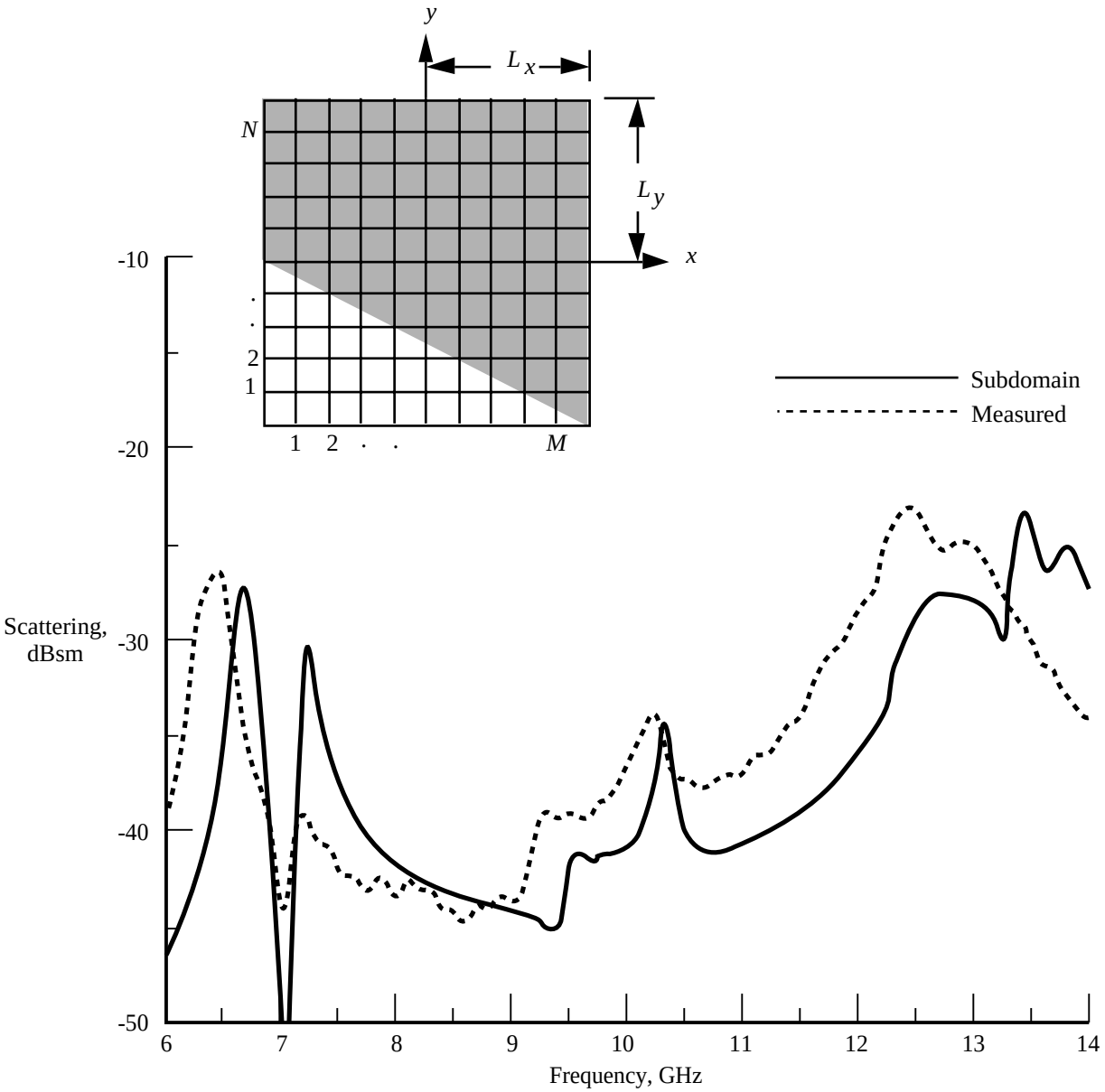

Figure 6. Comparison between subdomain and measured scattering from a trapezoidal microstrip patch antenna. $L_x = 0.7$ cm; $L_y = 1.4$ cm; $d = 0.07874$ cm; $\varepsilon_r = 2.33$; Loss tangent $= 0.001$; θ^i, $\phi^i = 60°, 180°$.